Ion-Pair Association in Ultrasupercritical Aqueous Environments: Successful Interplay among Conductance Experiments, Theory, and Molecular Simulations†

Ariel A. Chialvo,* Miroslaw S. Gruszkiewicz, and David R. Cole

Chemical Sciences Division, Geochemistry and Interfacial Science Group, Oak Ridge National Laboratory, Oak Ridge, Tennessee 37831-6110

We discuss the interplay among theory, molecular simulations, and electric conductance experiments as an important tool for the extraction of ion-pair interaction potentials to make possible the bridging of the density gap between the lowest experimentally attainable conductance measurement and the theoretically acceptable zero-density limit of the ion-pair association constant. The density dependence of the $Na^+\cdots Cl^-$ pair association constant in ultrasupercritical (USC) steam environments is predicted by a constraint molecular dynamics simulation over state conditions relevant to the new generation of USC steam power plants. Finally, we draw attention to relevant modeling challenges associated with the behavior of these systems around the zero-density limit, discuss ways to overcome the drawbacks of traditional $\log K_a - \log \rho$ models, and illustrate the case with an explicit quartic $(\rho)^{1/2}$-polynomial representation for $\log K_a$.

1. Introduction

The new generation of steam power plants targets ≈ 45 % efficiency by raising its operating conditions up to 760 °C and 37.9 MPa,[1] that is, into the regime of the so-called ultrasupercritical (USC) steam. The need for these rather extreme operating conditions is the result of increasingly larger energy demand and simultaneously more stringent environmental requirements toward the substantial reduction of CO_2 emissions.

USC aqueous solutions are obviously extreme environments characterized by relatively small dielectric permittivities whose thermophysical and chemical properties are exceptionally difficult to measure and, consequently, not well-understood.[2,3] Therefore, we are confronted with at least two important issues when dealing with processes involving USC environments: (a) the presence of even trace levels of ionic species from water impurities or chemical additives might trigger undesirable solid deposition,[4] and (b) the aqueous chemistry resulting from the interaction of USC steam with solid substrates, with metal corrosion as a potential consequence, is either mostly unknown or poorly understood.[5]

To appreciate the relevance of these two issues in the context of energy production, we must recall that our ability to control the chemistry of the steam cycle can have a profound impact on the ion-association equilibria, corrosion rate, solids deposition, and the potential manipulation of dissolution−precipitation processes. Furthermore, to understand the process of formation and stability of metal oxide layers (i.e., corrosion), we must account accurately for the actual species present whose chemistry depends directly on the thermophysical properties of the USC steam at the inhomogeneous solid−fluid interfacial region. To fulfill this requirement, we must develop predictive tools and experimental techniques able to capture ion speciation.

The two most frequently used approaches for the description of high temperature/pressure aqueous electrolytes solutions are equations of state (EoS) and empirical engineering correlations,[6] though neither one by itself has been successful in modeling the speciation behavior of simple aqueous electrolytes solutions. Typically the high-temperature EoS representations of simple aqueous systems invoke negligible contributions from speciation (i.e., all ions are assumed as paired entities),[6−8] and consequently, their heat of dilution predictions are rather poor.[9,10] This outcome has prompted the (empirical, ad hoc, or otherwise) incorporation of association models into the Anderko−Pitzer EoS[7] to account for ion speciation in the thermodynamic descriptions of low-dielectric aqueous electrolyte systems.

Regardless of the chosen thermodynamic modeling approach, its reliability as an accurate descriptor of ion speciation in aqueous electrolyte systems will depend crucially on the validity of the underlying hypotheses and approximations,[9,11,12] and consequently, we must have or provide tools to either validate them or guide their selection. With these in mind the ultimate objective was to develop and apply an approach encompassing the interplay among electric conductance measurements, theory, and molecular-based simulations to predict the ion-pair association behavior in USC steam over a wide range of solvent densities, including the zero-density limit. In its pursuit we will (a) discuss the adequacy (or lack thereof) of available parametrization of the ion-pair force fields to describe the actual ion-pair behavior in steam, (b) use the resulting optimized force-field parametrization to study the ion-pair association along USC isotherms, (c) discuss the failure of primitive models based on dielectrically screened electrostatics in the description of ion-pair association in steam environments, and finally (d) highlight some challenging features in the isothermal-density behavior of the ion association in extreme steam environments that make accurate modeling more difficult.

To address these tasks we first discuss in Section 2 our philosophy behind the interplay among electric conductance, theory, and simulations, including some outstanding issues with current ion-pair force fields. In Section 3 we present a brief description of the simulation method underlying the molecular-based prediction of ion-pair association constants and discuss the parametrization of the ion-pair force field. Then, in Section 4 we present the predicted isothermal-density behavior of the

† Part of the "Josef M. G. Barthel Festschrift".

* To whom correspondence should be addressed. E-mail: chialvoaa@ornl.gov. Fax: 865-574-4961.

10.1021/je900788r
Published on Web 03/01/2010

$Na^+\cdots Cl^-$ ion-pair association density results with a discussion of some relevant findings. We conclude in Section 5 with some observations about outstanding issues regarding the modeling of these challenging systems and what the future holds.

2. Interplay among Electrical Conductance, Theory, and Molecular Simulations

The pioneering experimental work on ion association in steam by Ölander and Liander,[13] Sourirajan and Kennedy,[14] Martynova et al.,[15−17] Khaibullin and Borisov,[18] Styrikovich et al.,[19] Lukashov et al.,[20] and the more recent studies of Pitzer,[11,21,22] Alekhin and Vakulenko,[23] and Bischoff et al.[24] among others, have provided a wealth of data for correlation purposes. Traditionally, this experimental information has been gathered from solubility measurements[13−19,25] and electric conductance measurements of dilute alkali halides.[20,26−30] The latter provides a direct route to the association constant usually supplemented by calorimetric,[31,32] isopiestic,[33,34] and volatility measurements[35,36] to facilitate the interpretation of the observed behavior. With the recent advances in the electric conductance methodology involving flow-through cells,[30,37] the association behavior for alkali halides at liquid-like densities can be considered well-established.[30,38,39] However, our understanding of the speciation phenomena for these electrolytes at low subcritical densities is still rather deficient, because this region has been typically unattainable by most experimental methodologies[40] and generally most measurements provide little insight into the system's microscopic behavior.[41]

In search for such a molecular-level understanding we have demonstrated over the years how molecular simulations of high temperature/pressure aqueous electrolyte solutions can be used to shed light on the ion association phenomena and provide accurate predictions of the corresponding constants.[3,42−47] In fact, molecular simulation has become an unmatched tool for the full characterization of the dielectric behavior of aqueous electrolyte solutions and their solvation microstructure and, consequently, the evaluation of ion-pair formation whose molecular-based interpretation will ultimately guide the development of successful macroscopic correlations.[48,49]

As we have recently argued,[3] the new design of the flow-through electric conductance apparatus is the most versatile and promising tool currently available to constrain the speciation characterization of USC steam environments. This technique allows for electric conductance measurements at ion concentrations as low as 10^{-6} mol·kg^{-1} (below 10^{-7} mole fraction) and, because of the extremely low ionic strengths, the determination of the corresponding ionic mobilities without the need for questionable extrapolation of the results obtained at higher concentrations. To take full advantage of these new capabilities and simultaneously retrieve accurate microscopic information about ions in steam environments that are essential for the ultimate development of molecular-based engineering modeling of USC systems, we have recently suggested and implemented an integrated molecular simulation-electric conductance approach.[3]

The main idea behind the interplay hinges around the parametrizations of the force field for the steam-mediated $Na^+\cdots Cl^-$ interactions, which are able to describe the corresponding association constant at the two extreme solvent environments for which we have reliable data. These are the zero-density limit (i.e., the condition where the aqueous environment behaves as an ideal gas system for which we have the JANAF tables;[50] for a detailed description of the ideal-gas ion-pairs please see the Pitzer's pioneering work[11]) and the liquid-like densities (for which we have data from our own electric conductance-based measurements[30,51]). To bridge the gap between the zero-density limiting-behavior of the association constant K_a for a salt M^+X^-, determined through the JANAF tabulations,[50] and that corresponding to the lowest density conditions accessible to current conductance experiments, we invoke the following limiting behavior,[46]

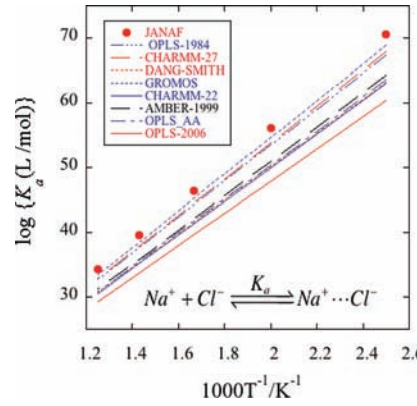

Figure 1. Comparison between the predicted temperature dependence of the $Na^+\cdots Cl^-$ pair association in the ideal gas limit by currently available models and the JANAF tabulated values. The identification of the force fields follows the acronyms given by Patra and Karttunen.[52] From top to bottom: JANAF, GROMOS, CHARMM-27, OPLS-84, AMBER-1999, OPLS-AA, DANG-SMITH, CHARMM-22, and OPLS-2006.

$$\lim_{\rho\to 0} K_a = K_a^{IG} = 4\pi \exp[-\phi_{M^+X^-}(r_2)/kT\varepsilon_0]\cdot \int_0^{r_2} \exp\{\int_0^r f_{M^+X^-}(r', \rho = 0) r^2\, dr'/kT\} r^2\, dr \quad (1)$$

where the superscript IG denotes the "ideal gas" solvent, $\phi_{M^+X^-}(r_2)$ is the direct intermolecular interaction for the ion pair at the point of anchorage r_2, and $f_{M^+X^-}(r,\rho)$ represents the mean force exerted on the ion pair separated by a distance r when surrounded by a zero-density solvent resulting in a dielectric constant $\varepsilon_0 = 1$.

Despite the existence of numerous sets of force-field (Lennard−Jones) parametrizations for the $Na^+\cdots Cl^-$ pair,[52] they mostly fail to predict the temperature dependence of the zero-density (ideal gas solvent) association constant, $K_a^{IG}(T)$, according to the values in the JANAF tables[50] as illustrated in Figure 1. Although this failure might appear as a setback, it actually creates an opportunity to direct the optimization of the ion pair's Lennard−Jones parameters to accurately predict $K_a^{IG}(T)$. The result of this optimization is shown in Figure 2 where we plot the curve of the optimized Lennard−Jones parameters ε_{NaCl}/k versus σ_{NaCl} together with the corresponding sets based on currently used parametrization from the literature.[52] This comparison indicates for example that, with the exception of AMBER-1999[53] and GROMOS[54] whose force fields fall close to the optimized values, most known parametrizations for $\phi_{NaCl}(r)$ exhibit considerable scatter within the $\varepsilon_{NaCl}/k - \sigma_{NaCl}$ plane. This outcome can be better understood if we recall that individual parametrizations usually target different properties during the regression process (including solvation free energies[55] and hydration numbers[56] at normal conditions), that is, we should not expect them to become fully transferable force fields. More importantly, the suggested optimization does not provide just a unique value for the force-field pair, but a continuum function $\varepsilon_{NaCl}/k = J(\sigma_{NaCl})$, that is, the optimized Lennard−Jones parameters are coupled in a way that all (ε_{NaCl}/k, σ_{NaCl}) pairs along the optimized curve will collapse (within the numerical uncertainties of the calculations) into the same total ion-pair

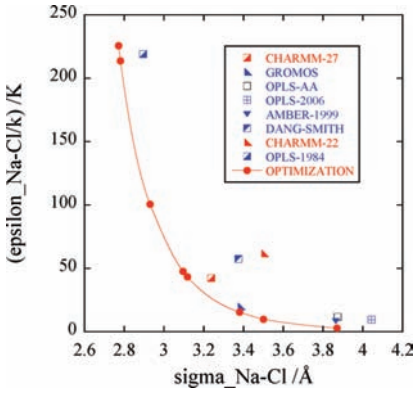

Figure 2. Optimized energy and size parameters for the $Na^+\cdots Cl^-$ pair interactions in comparison with those from currently available models also plotted in Figure 1.

potential $\phi_{NaCl}(r) = u_{LJ}(r) + u_{Coul}(r)$ as illustrated in Figure 3a−c. In particular, note the significant disparate predictions by the current models for the location and magnitude of the minimum of $\phi_{NaCl}(r)$ in comparison with our optimized profile, Figure 3a, which can be traced back to the corresponding Lennard−Jones parametrizations. In fact, as we illustrate in Figure 3b, the Lennard−Jones portion of most currently available $Na^+\cdots Cl^-$ pair potentials[52] describes rather disparate interaction strengths. In that sense the optimized curve $\varepsilon_{NaCl}/k = J(\sigma_{NaCl})$ depicted in Figure 2 exhibits a similar behavior with an important caveat as shown in Figure 3c, that is, each of the optimized Lennard−Jones potentials collapses into a single $\phi_{NaCl}(r)$ curve when added to the corresponding Coulombic contributions.

Clearly, the issue here is how to select a particular force-field set from the optimized curve, that is, one that could simultaneously predict accurately not only $K_a^{IG}(T)$ but also the corresponding $K_a(T, \rho > 0)$, where the latter involves both the direct and the steam-mediated ion-pair interactions. These steam-mediated interactions, described in terms of ion−solvent pair potentials, are typically estimated as (geometric, arithmetic, or a combination of both) mean values of the corresponding ion−ion and solvent−solvent parameters (i.e., the so-called combining rules).

The procedure we have used here is as follows. Because the Lennard−Jones parameters for the Cl−Cl pair interactions are the most consistently obtained (smaller variability) in the literature,[52] we use this pair in conjunction with the JANAF-based optimized Na−Cl pair and the conventional Lorentz−Berthelot combining rules to estimate the remaining Lennard−Jones parameters for the O−Cl and the O−Na interactions that will predict $K_a(T, \rho > 0)$ in close agreement with that from our electric conductivity measurements.[30] After a few trials[57] involving the TIP4P-2005 water model[58] we chose the parameter sets given in Table 1.

3. Molecular-Based Prediction of Ion-Pair Association Constants

The first ingredients needed for the prediction of ion-pair association are, as discussed in the previous section, the properly parametrized force fields for the precisely defined model system representing an infinitely dilute aqueous electrolyte solution. The simulation approach for the prediction of ion-pair association constants has been extensively described elsewhere[42,44,45,59] (for a comprehensive recent review on ion association in supercritical aqueous systems also see Guardia et al.[60]). Basically, this molecular-based route provides the radial profiles of the infinitely dilute ion-pair potential of mean force (PMF), whose volume integration defines the association constant and the corresponding equilibrium constant between ion-pair configurations (see for example Appendix A of ref 45). Moreover, to assess explicitly the "solvent effect" on the strength of the ion-pair association we utilize eq 1 to calculate the isothermal ratio $(K_a/K_a^{IG})_T$,

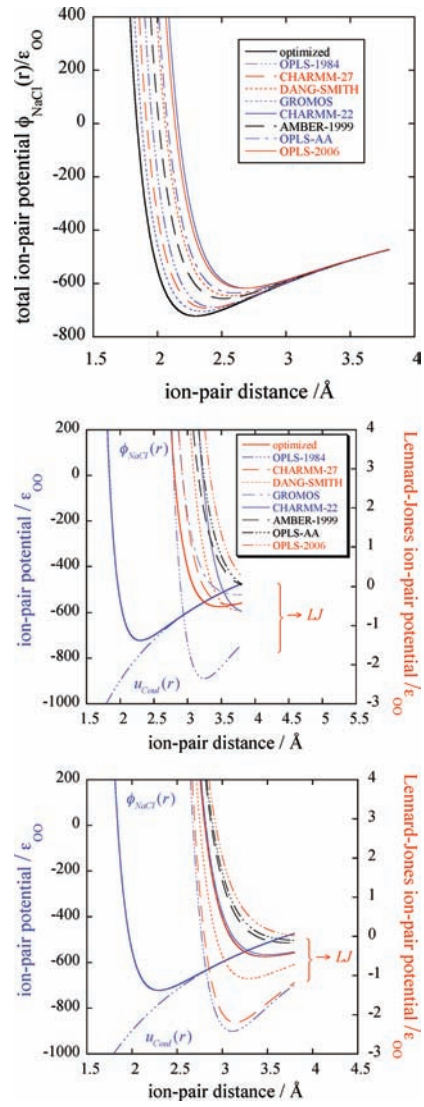

Figure 3. (a) Radial dependence of the total $Na^+\cdots Cl^-$ pair potentials, $\phi_{NaCl}(r) = u_{LJ}(r) + u_{Coul}(r)$, as predicted by currently available models in comparison with the optimized one. From right to left: optimized, GROMOS, CHARMM-27, OPLS-84, AMBER-1999, DANG-SMITH, OPLS-AA, OPLS-2006, and CHARMM-22. (b) Lennard−Jones pair potential contributions as predicted by available force fields in comparison with the corresponding Coulombic and optimized total potentials and (c) Lennard−Jones pair potential contributions as predicted by the optimized Lennard−Jones pair potentials of Figure 2 in comparison with the corresponding Coulombic and optimized total potentials. Each LJ-labeled curve corresponds to a particular $\sigma_{NaCl} - \varepsilon_{NaCl}$ pair along the optimized curve from Figure 2. The addition of any of these $u_{LJ}(r)$ curves to the Coulombic term $u_{Coul}(r)$ collapses into the same $\phi_{NaCl}(r)$ (thick line).

Table 1. Lennard−Jones Parameters Used in This Work

pair interaction	ε_{ij}/k/K	σ_{ij}/Å
NaCl[a]	47.7	3.096
ONa	62.9	2.459
OCl	70.68	3.779

[a] JANAF-based optimization.

$$\frac{K_a}{K_a^{IG}} = \exp\left[-\frac{\varphi_{M^+X^-}(r_2)(\varepsilon^{-1} - \varepsilon_0^{-1})}{kT}\right] \cdot \left[\frac{\int_0^{r_2} \exp\{\int_{r_2}^{r} f_{M^+X^-}(r', \rho) r^2 \, dr'/kT\} r^2 \, dr}{\int_0^{r_2} \exp\{\int_{r_2}^{r} f_{M^+X^-}(r', \rho = 0) r^2 \, dr'/kT\} r^2 \, dr}\right] \quad (2)$$

through the determination of radial profiles of the mean force, $f_{M^+X^-}(r, \rho)$, and the explicit evaluation of the dielectric constant of the pure solvent, ε, at the prevailing state conditions.

In this assessment we conducted isothermal−isochoric molecular dynamics simulations involving 254 water molecules and the ion pair, along three USC isotherms, that is, $T =$ (1073, 1173, and 1273) K, and within the density range of $0.0 \leq \rho$ (g·cm^{-3}) ≤ 0.80, according to the methodology described elsewhere.[44,45] Each state condition required 40 to 45 constraint-dynamics runs, whose trajectories spanned between (0.4 and 1.6) ns after equilibration to calculate the time averages of the ion−ion and solvent-induced ion-pair contributions to the mean force, as well as the equivalent constraint-force counterpart.[61]

For illustration purposes in Figure 4 we display the simulated profiles for the two contributions to the $Na^+\cdots Cl^-$ mean force and the resulting PMF at the USC condition of $\rho = 0.6$ g·cm^{-3} and $T = 1273$ K. The equivalence between the two mean-force approaches, that is, "blue-moon" versus "constraint-force", is clearly substantiated on the top of Figure 4 and confirms the internal consistency of the resulting profiles. By integration of the mean-force profiles we subsequently obtain first the PMF's and, after invoking eqs 1 and 2, the corresponding K_a as described in detail in ref 46.

In the lower part of Figure 4 we also include a direct comparison between the actual PMF profile and that predicted by the primitive model counterpart based on a continuum dielectric solvent (i.e., the so-called Born approximation[62]), characterized by the dielectric permittivity of the model steam that attenuates the electrostatic $Na^+\cdots Cl^-$ pair interactions. This comparison features the typical shape of the PMF profiles, that is, exhibiting (a) a well-defined first valley and a subtler second valley describing the contact ion pair (CIP) and the steam-shared ion pair (SShIP) configurations, respectively, when involving the explicit atomistic description of the steam, and (b) a single valley shifted toward larger contact ion-pair distances and the asymptotic approach to the explicit-steam PMF profile for ion-pair distances beyond that of the SShIP. The modeling implications of this behavior will be addressed in the Discussion Section below.

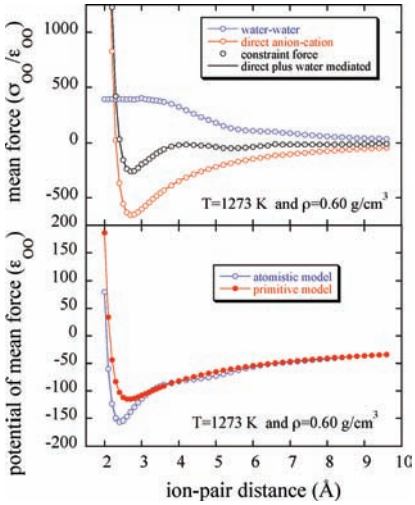

Figure 4. Radial profile of (a) the direct and solvent-mediated contributions to the mean force and the corresponding constraint-force counterpart and (b) the resulting PMF in comparison with the corresponding primitive model for the $Na^+\cdots Cl^-$ pair at $T = 1273$ K and $\rho = 0.6$ g·cm^{-3}.

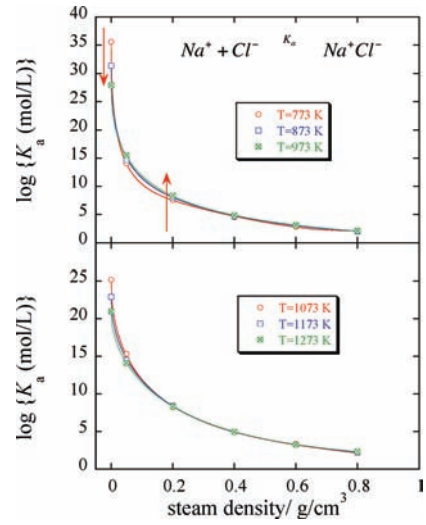

Figure 5. Density dependence of the $Na^+\cdots Cl^-$ pair association constant along six supercritical isotherms. Arrows in (a) indicate the direction of increasing temperature to highlight the occurrence of a crossover between $0 < \rho < 0.05$ g·cm^{-3}. Lines are given by the fitting expressions 8 and 9 discussed in the main text.

4. Discussion of Simulation Results

In this section we discuss the predicted isothermal-density and isochoric-temperature behavior of the $Na^+\cdots Cl^-$ pair association constant and the corresponding degrees of dissociation in USC steam environments. For comparison purposes we also consider some recently reported data along three other USC isotherms to highlight some relevant features including the change of the isothermal-density dependence, the occurrence of a temperature crossover, and its modeling implications.

In Figure 5 we compare the predicted density dependence of $\log K_a$ along two sets of USC isotherms, that is, $773 \leq T/\text{K} \leq 973$ from our previous work[3] and $1073 \leq T/\text{K} \leq 1273$ from the current work. There are two significant features in this figure: (a) the obvious strong isothermal-density dependence exhibited by $\log K_a$, that is, a change of about 20 to 35 orders of magnitude as the steam density increases from (0.0 to 0.8) g·cm^{-3}, and (b) the presence of an isochoric-temperature crossover for the isotherms $773 \leq T/\text{K} \leq 973$, described as a change of sign in the isochoric temperature-derivative $(\partial \log K_a/\partial T)_\rho$ at $\rho^\times \approx 0.04$ g·cm^{-3}, and its apparent absence for the isotherms in the range $1073 \leq T/K \leq 1273$. Interestingly, we should note that Liu et al.[2] have also predicted such a crossover through the modeling of their ab initio free energy perturbation simulations of five state points along the 723 K and 973 K isotherms (see their Figure 4). Although we can confirm the occurrence of the crossover, we have no molecular or other basis to either support or justify the existence of a unique crossover point, that is, at $\rho^\times$.

To gain some understanding of such a peculiar behavior, we display the isochoric-(inverse) temperature dependence of $\log K_a$ in Figure 6 along the six studied densities. It becomes immediately clear that these isochors exhibit quasi-linear T^{-1} dependence whose slopes go from flat or slightly negative, $(\partial \log K_a/\partial T^{-1})_\rho \leq 0$ at liquid-like densities, to strongly positive $(\partial \log K_a/\partial T^{-1})_\rho > 0$ for the zero-density limit. Moreover, the transition between these two extreme cases manifests as a slight curvature of the originally quasi-linear behavior clearly seen for the $\rho = 0.05$ g·cm^{-3} isochor (this feature will be illustrated

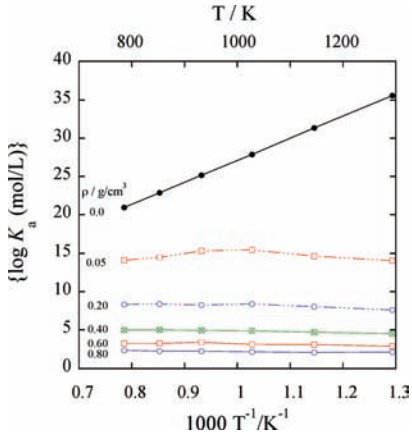

Figure 6. Isochoric-temperature dependence of the $Na^+\cdots Cl^-$ pair association constant at USC conditions from simulation.

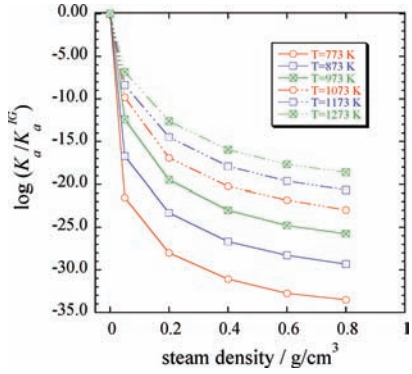

Figure 7. Isothermal-density dependence of the $Na^+\cdots Cl^-$ pair association constant relative to the corresponding zero-density limit K_a^{IG}.

further in the final section below). This transition between positive and negative slopes would imply that the alleged crossover must occur over the entire range of temperatures under investigation. The fact that we do not apparently capture it in the predictions of Figure 5b has to do with the relatively small isochoric-temperature or isothermal-density effect on log K_a around the crossover density.

Because USC steam typically exhibits a relatively low dielectric permittivity, a recurrent question concerns the actual solvation power of steam, that is, its ability to keep the ion pair dissociated at these extreme environments. To gain insight into the behavior of steam as a solvent, and subsequently to answer the previous question, we first use eq 2 to assess the solvent effect on the K_a along USC isotherms as illustrated in Figure 7. These isotherms can then be reinterpreted in terms of the degree of ion-pair dissociation, α, and its relative strength with respect to the corresponding ideal-gas solvent counterpart, α^{IG}, as illustrated in Figure 8a,b for a total salt concentration of 10^{-6} mol·L^{-1}.

Figure 7 indicates that the buildup of steam density along USC isotherms has a substantially large effect on the relative stability of the individual ions that translates into a (7 to 23) orders of magnitude enhancement of the association constant over that of the corresponding ideal gas counterpart, when the steam density reaches 0.05 g·cm^{-3} within the range of USC isotherms. Note that this enhancement is comparable to that corresponding to the systems when the steam density is increased from 0.05 g·cm^{-3} to the liquid-like value of 0.8 g·cm^{-3}. The significance of such a behavior becomes highlighted in Figure 8a,b, where the zero-density limit $Na^+\cdots Cl^-$ pairs are fully associated CIPs, that is, $\alpha < 10^{-7}$ (top graph),

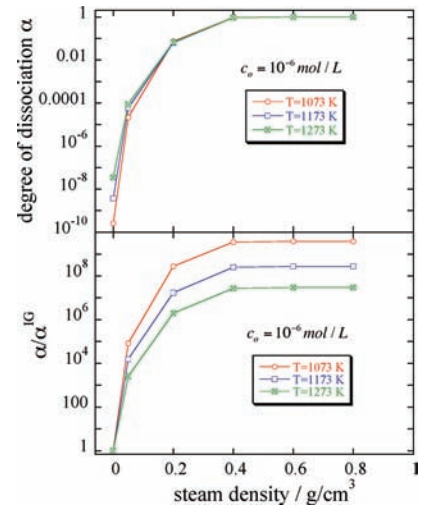

Figure 8. Density dependence of (a) the degree of $Na^+\cdots Cl^-$ pair dissociation along three USC isotherms and (b) their ratio to the corresponding ideal-gas counterpart for a total salt concentration $c_o = 10^{-6}$ mol·L^{-1}.

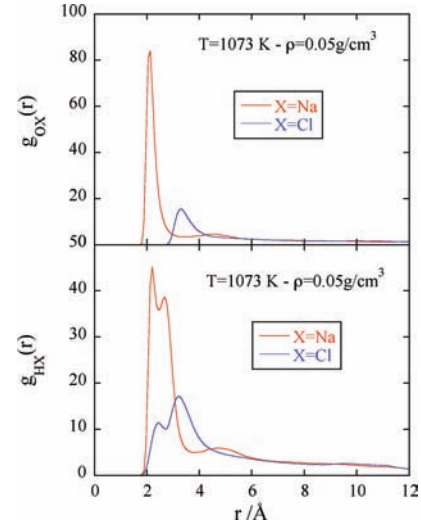

Figure 9. Comparison between the steam local environment around the free ion and counterion at infinite dilution in terms of the corresponding radial distribution functions of the ion−water site interactions at $T = 1073$ K and $\rho = 0.05$ g·cm^{-3}.

while an increase of just 0.05 g·cm^{-3} from that limiting condition translates into a 10^3 to 10^5 enhancement of the ion-pair dissociation for $1073 \leq T/K \leq 1273$ (bottom graph). In comparison, the corresponding enhancement along $773 \leq T/K \leq 973$ is about 10^6 to 10^{10} as illustrated elsewhere,[3] that is, an indication of the remarkable solvation power exhibited by steam even at these extreme steam conditions and the origin of most modeling difficulties.

The solvation behavior of the dissociated pair at a representative extreme condition is clearly depicted in Figure 9 in terms of the radial distribution functions for the ion−water interactions. By recalling the formal definition of these distribution functions as $g_{IO}^{\infty}(r) = \rho_{IO}^{\infty}(r)/\rho_O^{bulk}$ we can conclude that the relative stability of the dissociated ion pairs are linked to the rather strong interactions of the ions with the steam that gives rise to significant inhomogeneous local steam density around the ions, that is, strong hydration, that hinders the close encounter of ion−counterion and potential formation of ion pairs. It is precisely this ion solvation behavior that works against the use of dielectric-based models for the description and interpretation

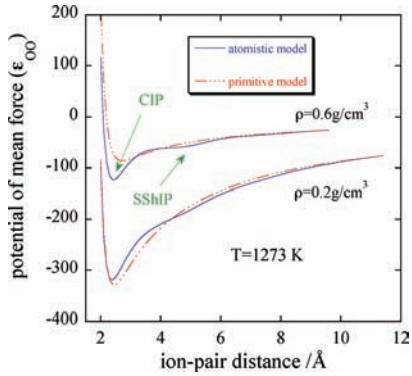

Figure 10. Comparison of the PMF radial profiles between the actual system with explicit description of the steam environment and the corresponding primitive solvent counterpart at $T = 1273$ K for densities $\rho = 0.6$ g·cm^{-3} and $\rho = 0.2$ g·cm^{-3}.

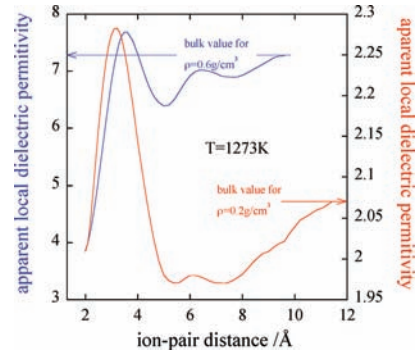

Figure 11. Profile of the apparent dielectric permittivity of steam required by the primitive model to predict accurately the association constant along $T = 1273$ K at two different bulk steam densities.

of ion-pair association in aqueous (and particularly steam) environments. Because these primitive models portray the steam environment implicitly as a uniform continuum dielectric, where the ion−counterion Coulombic interactions are accounted for by dielectrically screened electrostatics and usually without excluded volume contributions, they are not consistent with the physical reality depicted by Figure 9. Central to such behavior are the steam compressibility, the concomitant strong ion electrostriction, and the potential dielectric saturation that cannot be ignored in the modeling of these extreme environments.[46,63] In fact, earlier permittivity measurements[64] confirmed the local alteration of the solvent dielectric near ions that translates into a change in the equilibrium ion-pair distance and, consequently, a change in the strength of the resulting dipole moment. On the basis of these observations, Barthel[65] proposed a semiphenomenological modeling approach to ion-pair association with the inclusion of short-range interactions for which the "fully electrostatic" models of Fuoss[66] and Bjerrum,[67] as well as their modifications,[68] become special cases, that is, when invoking infinite dilution and no short-range excluded volume interactions.

Note that, even when including the short-range van der Waals interactions in the description of the ion-pair PMF, the use of the primitive model (embodied in the dielectrically attenuated electrostatic interactions) provides a significantly inaccurate prediction for the ion-pair association constant in steam media. For instance, in Figure 10 we illustrate this point by comparing the predicted ion-pair PMF at 1273 K for a liquid-like and a steam-like density according to the atomistic and primitive description of the aqueous environment. In addition to the obvious stabilization of the CIP configuration (at $\approx$ 2.4 Å) with decreasing steam density, this picture highlights (a) the presence of a weak SShIP at $\approx$ 4.3 Å, (b) the inability of the primitive model to account for an SShIP configuration, and (c) the failure to predict the proper location and strength of the CIP configuration.

Alternatively, through consideration of the Born-type equations,[69] we can ask what the field-dependent, as opposed to the uniform, dielectric permittivity should look like for the primitive model in Figure 10 to agree with the corresponding atomistic model predictions, that is, the profile $\varepsilon_{\text{apparent}}(r)$ that satisfies the condition $\text{PMF}(r) = u^{\text{LJ}}_{\text{NaCl}}(r) - e^2/r\varepsilon_{\text{apparent}}(r)$. This issue is addressed in Figure 11, where the oscillatory behavior of the calculated "apparent" dielectric profile follows closely the location of the ion-pair configurations, where the actual polarization does not respond to the homogeneous environment invoked by the Born equation. Note however that, by construction, the predictions of this atomistic model approach asymptotically those of the corresponding primitive models at the zero-density limit (see eqs 1 and 2).

5. Final Remarks

We integrated the use of theory, molecular simulations, and electric conductance measurements (available at liquid-like density conditions) for the extraction of accurate ion-pair interaction potentials for the prediction of association constants within the region of state conditions that are currently unattainable by electric conductance experiments. Extensive molecular dynamics simulations were performed to predict the isochoric-temperature and isothermal-density behavior of the $Na^+\cdots Cl^-$ pair association constant in extreme steam environments and bridge the density gap between the lowest experimentally attainable conductance measurement and the theoretically reachable zero-density limit of the ion-pair association constant.

The simulation results highlighted some relevant modeling challenges related to the peculiar behavior of these systems around the zero-density limit, in particular, the occurrence of a temperature crossover. The crossover behavior discussed and illustrated in Figures 5 and 6 represents a challenging feature to account for in the macroscopic modeling of ion association in steam. The traditional $\log K_a$−$\log \rho$ representations of the association isotherms[11,28,30,40,70,71] cannot accommodate the observed temperature crossover and describe simultaneously the zero-density limit predicted from the JANAF tables. To emphasize this point we considered the following conventional description,[40]

$$\log K_a = A + B/T + (C - D/T)\log \rho \qquad (3)$$

and set the necessary conditions for the alleged crossover to occur at $\rho = \rho^\times$, that is,

$$\log K_a(T_n, \rho^\times) = \log K_a(T_{n+1}, \rho^\times) \equiv \log K_a^\times \quad \text{for any } n \qquad (4)$$

$$(\partial \log K_a/\partial T)_{T_n,\rho^\times} = (\partial \log K_a/\partial T)_{T_{n+1},\rho^\times} \quad \text{for any } n \qquad (5)$$

According to eq 3, eqs 4 and 5 are simultaneously satisfied when the coefficients B and D are linked by the following condition,

$$B/D = \log \rho^\times \qquad (6)$$

Thus, under these constraints, eq 3 reduces to the following regression expression,

$$\log K_a = \log K_a^\times + (C - D/T)\log(\rho/\rho^\times) \qquad (7)$$

where $\log K_a^\times$ is given by eq 4. In summary, eq 7 will provide an expression to regress experimental data exhibiting the alleged

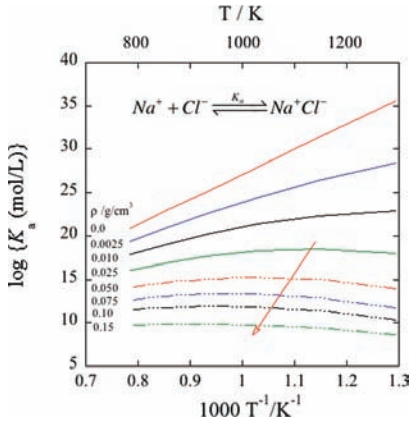

Figure 12. Predicted isochoric-temperature dependence of the $Na^+\cdots Cl^-$ pair association constant at USC conditions according to the regression of simulation results by eq 8. Arrow indicates the shift of the location of $(\partial \log K_a/\partial T^{-1})_\rho = 0$.

crossover. Note however that eq 7 or any alternative involving a logarithmic dependence on a vanishing variable is unsuitable for handling the zero-density limit and, consequently, of little use for the current analysis of low-density steam environments as already discussed elsewhere.[3,46]

Inspired by the cubic-spline interpolation scheme used recently by Liu et al.[2] we propose a well-behaved (particularly as $\rho \to 0$) and rather flexible quartic $(\rho)^{1/2}$-polynomial representation for the ion-pair association constant in USC steam environments, that is,

$$\log K_a = a(T) + b(T)\rho^{0.5} + c(T)\rho + d(T)\rho^{1.5} + e(T)\rho^2 \tag{8}$$

with the following temperature dependence for the density coefficients,

$$\xi(T) = \xi_o + \xi_1 T^{-1} + \xi_2 T^{-2} \quad \text{for} \quad \xi = (a, b, c, d, e) \tag{9}$$

so that,

$$\log K_a^{IG} = a(T) \tag{10}$$

For illustration purposes only, we regressed our simulation results through the proposed quartic polynomial, eq 8, whose resulting fit is represented by the lines in Figure 5. On the basis of this regression, we can now highlight the evolution of the discussed slopes $(\partial \log K_a/\partial T^{-1})_\rho$ of Figure 6, along isochores near the zero-density limit. For example, we note that $(\partial \log K_a/\partial T^{-1})_\rho$ is always positive for steam densities $\rho < 0.015$ g·cm^{-3} and exhibits a positive-to-negative smooth transition (that is, the condition for the existence of a temperature crossover) for $\rho > 0.01$ g·cm^{-3}. As the steam density approaches liquid-like values, this transition becomes less evident as the $\log K_a - T^{-1}$ relationship turns into a quasi-linear representation with a very small negative slope (see Figure 12).

While the existence of this crossover has an enthalpic (or entropic) interpretation whose significance can be exploited for modeling purposes,[3] it also suggests new questions regarding the underlying microscopic mechanism whose answers might provide insights toward the molecular-based understanding and subsequent successful engineering modeling of ion association in steam environments.

Finally, it is worth noting that similar ideas underlying the discussed approach can in principle be applied to UV−visible and IR spectroscopy.[72,73] Moreover, while here we utilized $Na^+\cdots Cl^-$ for illustration purposes, there are obviously other relevant ionic species involved in the chemistry of steam power generation and hydrothermal vents such as multivalent transition metal ions. Because these systems follow stepwise ion-pair formation, the proposed interplay could in principle be adapted for the same purposes, though it has not been attempted yet.

Acknowledgment

A.A.C. acknowledges illuminating discussions over the years with Robert E. Mesmer, J. Michael Simonson, Donald A. Palmer, William L. Marshall, and Robert H. Wood.

Literature Cited

(1) Moore, T. Coal-based Generation at the Crossroads. *EPRI J.* **2005**, 6–15.
(2) Liu, W. B.; Wood, R. H.; Doren, D. J. Sodium chloride in supercritical water as a function of density: Potentials of mean force and an equation for the dissociation constant from 723 to 1073 K and from 0 to 0.9 g/cm(3). *J. Phys. Chem. B* **2008**, *112* (24), 7289–7297.
(3) Chialvo, A. A.; Gruszkiewicz, M. S.; Simonson, J. M.; Palmer, D. A.; Cole, D. R. Ion Pair Association in Extreme Aqueous Environments: Molecular-based and Electrical Conductance Approaches. *J. Solution Chem.* **2009**, *38* (7), 827–841.
(4) Bellows, J. C.; Harvey, A. H. Steam solubilities for combustion turbine steam cooling. *Int. J. Thermophys.* **1999**, *20* (1), 197–205.
(5) Jonas, O. Water chemistry and corrosion in steam cycles - Missing knowledge. *Materials Perform.* **2003**, *42* (11), 32–36.
(6) Leusbrock, I.; Metz, S. J.; Rexwinkel, G.; Versteeg, G. F. Quantitative approaches for the description of solubilities of inorganic compounds in near-critical and supercritical water. *J. Supercrit. Fluids* **2008**, *47* (2), 117–127.
(7) Anderko, A.; Pitzer, K. S. Equation-of-State Representation of Phase-Equilibria and Volumetric Properties of the System NaCl-H_2O above 573-K. *Geochim. Cosmochim. Acta* **1993**, *57* (8), 1657–1680.
(8) Kosinski, J. J.; Anderko, A. Equation of state for high-temperature aqueous electrolyte and nonelectrolyte systems. *Fluid Phase Equilib.* **2001**, *183*, 75–86.
(9) Liu, B.; Oscarson, J. L.; Peterson, C. J.; Izatt, R. M. Improved thermodynamic model for aqueous NaCl solutions from 350 to 400 degrees C. *Ind. Eng. Chem. Res.* **2006**, *45* (9), 2929–2939.
(10) Oscarson, J. L.; Palmer, B. A.; Fuangswasdi, S.; Izatt, R. M. A New Model Incorporating Ion Dissociation for Sodium Chloride Solutions near the Critical Point of Water. *Ind. Eng. Chem. Res.* **2001**, *40*, 2176–2182.
(11) Pitzer, K. S. Thermodynamics of Sodium Chloride Solutions in Steam. *J. Phys. Chem.* **1983**, *87*, 1120–1125.
(12) Sue, K.; Adschiri, T.; Arai, K. Predictive model for equilibrium constants of aqueous inorganic species at subcritical and supercritical conditions. *Ind. Eng. Chem. Res.* **2002**, *41* (13), 3298–3306.
(13) Ölander, A.; Liander, H. The Phase Diagram of Sodium Chloride and Steam above the Critical Point. *Acta Chem. Scand.* **1950**, *4*, 1437–1445.
(14) Sourirajan, S.; Kennedy, G. C. The System H_2O-NaCl at Elevated Temperatures and Pressures. *Am. J. Sci.* **1962**, *260*, 115–141.
(15) Martynova, O. I.; Samoilov, Y. F. The Formation of Solutions of Inorganic Substances in Water Vapour. *Russ. J. Inorg. Chem.* **1962**, *7*, 372–375.
(16) Martynova, O. I. Some Problems of the Solubility of Involatile Inorganic Compounds in Water Vapour at High Temperatures and Presures. *Russ. J. Phys. Chem.* **1964**, *38*, 587–592.
(17) Martynova, O. I.; Smirnov, O. K. Solutions of Inorganic Compounds in Supercritical Steam. *Russ. J. Inorg. Chem.* **1964**, *9*, 145–149.
(18) Khaibullin, K.; Borisov, N. M. Experimental Investigation of the Thermal Properties of Aqueous and Vapor Solutions of Sodium and Potassium Chlorides at Phase Equilibrium. *High Temp. Sci.* **1966**, *4*, 518–523.
(19) Styrikovich, M. A.; Martynova, O. I.; Mingulina, E. I. The Dependence of the Coordination Number of Weak Electrolytes on the Density of the Solvent Water. *Dokl. Phys. Chem.* **1966**, *171*, 783–786.
(20) Lukashov, Y. M.; Komissarov, K. B.; Golubev, B. P.; Smirnov, S. N.; Svistunov, E. P. An Experimental Investigation of Electrolytic Properties of Uni-Univalent Electrolytes at High Parameters of State. *Therm. Eng.* **1975**, *22* (12), 89–92.
(21) Pitzer, K. S.; Li, Y.-G. Critical phenomena and thermodynamics of dilute aqueous sodium chloride to 823 K. *Proc. Natl. Acad. Sci. U.S.A.* **1984**, *81*, 1268–1271.
(22) Pitzer, K. S.; Palaban, R. T. Thermodynamics of NaCl in Steam. *Geochim. Cosmochim. Acta* **1986**, *50*, 1445–1454.

(23) Alekhin, Y. V.; Vakulenko, A. G. Thermodynamic Parameters and Solubility of NaCl in Water Vapor at 300−500 °C up to 300 bar. *Geochem. Int.* **1987**, *24* (10), 97–110.

(24) Bischoff, J. L.; Rosenbauer, R. J.; Pitzer, K. S. The System NaCl-H_2O: Relations of Vapor-Liquid Near the Critical Temperature of Water and of Vapor-Liquid-Halite from 300° to 500°C. *Geochim. Cosmochim. Acta* **1986**, *50*, 1437–1444.

(25) Galobardes, J. F.; Van Hare, D. R.; Rogers, L. B. Solubility of Sodium Chloride in Dry Steam. *J. Chem. Eng. Data* **1981**, *26*, 363–366.

(26) Quist, A. S.; Marshall, W. L. Electrical Conductances of Aqueous Sodium Chloride Solutions from 0 to 800 Degrees and at Pressures to 4000 Bars. *J. Phys. Chem.* **1968**, *72*, 684–703.

(27) Lukashov, Y. M.; Savenko, V. V. Experimental-Study of Physicochemical Properties of Salt, Acid, and Alkaline-Solutions in Deuterium-Oxide at Saturation Line. *Zh. Fiz. Khim.* **1980**, *54* (6), 1582–1584.

(28) Ho, P. C.; Palmer, D. A.; Mesmer, R. E. Electrical Conductivity Measurements of Aqueous Sodium Chloride Solutions to 600 deg C and 300 MPa. *J. Solution Chem.* **1994**, *23*, 997–1018.

(29) Zimmerman, G. H.; Gruszkiewicz, M. S.; Wood, R. H. New Apparatus for Conductance Measurements at High Temperature: Conductance of Aqueous Solutions of LiCl, NaCl, NaBr, and CsBr at 28 MPa and Water Densities from 700 to 260 kg/m3. *J. Phys. Chem.* **1995**, *99*, 11612–11625.

(30) Gruszkiewicz, M. S.; Wood, R. H. Conductance of LiCl, NaCl, NaBr, and CsBr Solutions in Supercritical Water Using a Flow Conductance Cell. *J. Phys. Chem. B* **1997**, *101*, 6549–6559.

(31) Piekarski, H. Application of Calorimetric Methods to Investigations of Interactions in Solutions. *Pure Appl. Chem.* **1999**, *71*, 1275–1283.

(32) Wachter, R.; Riederer, K. Properties of Dilute Electrolyte Solutions from Calorimetric Measurements. *Pure Appl. Chem.* **1981**, *53*, 1301–1312.

(33) Holmes, H. F.; Mesmer, R. E. An Isopiestic Study of Aqueous Solutions of the Alkali Metal Bromides at Elevated Temperatures. *J. Chem. Thermodyn.* **1999**, *30*, 723–741.

(34) Mesmer, R. E.; Palmer, D. A.; Simonson, J. M.; Holmes, H. F.; Ho, P. C.; Wesolowski, D. J.; Gruszkiewicz, M. S. Experimental Studies in High Temperature Aqueous Chemistry at Oak Ridge National Laboratory. *Pure Appl. Chem.* **1997**, *69*, 905–914.

(35) Palmer, D. A.; Simonson, J. M. Volatility of Amonium Chloride over Aqueous Solutions to High Temperatures. *J. Chem. Eng. Data* **1993**, *38*, 465–474.

(36) Simonson, J. M.; Palmer, D. A. Liquid-Vapor Partitioning of HCl(aq) to 350 °C. *Geochim. Cosmochim. Acta* **1993**, *57*, 1–8.

(37) Zimmerman, G. H.; Scott, P. W.; Greynolds, W. A new flow instrument for conductance measurements at elevated temperatures and pressures: Measurements on NaCl(aq) to 458 K and 1.4 MPa. *J. Solution Chem.* **2007**, *36* (6), 767–786.

(38) Ho, P. C.; Palmer, D. A. Determination of Ion Association in Dilute Aqueous Lithium Chloride and Lithium Hydroxide Solutions to 600 °C and 300 MPa by Electrical Conductance Measurements. *J. Chem. Eng. Data* **1998**, *43*, 102–110.

(39) Zimmerman, G. H.; Scott, P. W.; Greynolds, W.; Mayorov, D. Conductance of Dilute Hydrochloric Acid Solutions to 458 K and 1.4 MPa. *J. Solution Chem.* **2009**, *38* (4), 499–512.

(40) Mesmer, R. E.; Palmer, D. A.; Simonson, J. M. Ion Association at High Temperatures and Pressures. In *Activity Coefficients in Electrolyte Solutions*, 2nd ed.; Pitzer, K. S., Ed.; CRC Press: Boca Raton, 1991; pp 491−529.

(41) Palmer, D. A.; Simonson, J. M.; Jensen, J. P. Partitioning of Electrolytes to Steam and their Solubilities in Steam. In *Aqueous Systems at Elevated Temperatures and Pressures*; Palmer, D. A., Fernandez-Prini, R., Harvey, A. H., Ed.; Elsevier: London, 2004.

(42) Chialvo, A. A.; Cummings, P. T.; Cochran, H. D.; Simonson, J. M.; Mesmer, R. E. Na^+-Cl^- Ion Association in Supercritical Water. *J. Chem. Phys.* **1995**, *103*, 9379–9387.

(43) Chialvo, A. A.; Cummings, P. T. Molecular-based Modeling of Water and Aqueous Solutions at Supercritical Conditions. In *Advances in Chemical Physics*; Rice, S. A., Ed.; Wiley & Sons: New York, 1999; Vol. 109, pp 115−205.

(44) Chialvo, A. A.; Cummings, P. T.; Simonson, J. M. H_3O^+/Cl^- Ion Pair Formation in High-Temperature Aqueous Solutions. *J. Chem. Phys.* **2000**, *113*, 8093–8100.

(45) Chialvo, A. A.; Ho, P. C.; Palmer, D. A.; Gruszkiewicz, M. S.; Cummings, P. T.; Simonson, J. M. H_3O^+/Cl^- Association in High-Temperature Aqueous Solutions over a Wide Range of State Conditions. A Direct Comparison between Simulation and Electrical Conductance Experiment. *J. Phys. Chem. B* **2002**, *106*, 2041–2046.

(46) Chialvo, A. A.; Simonson, J. M. Aqueous Na^+Cl^- Pair Association from Liquid-like to Steam-like Densities along Near-critical Isotherms. *J. Chem. Phys.* **2003**, *118*, 7921–7929.

(47) Chialvo, A. A.; Simonson, J. M. $H_3O^+Cl^-$ pair association in steam and highly compressible aqueous environments. *J. Phys. Chem. C* **2007**, *111* (43), 15569–15574.

(48) Chialvo, A. A.; Cummings, P. T.; Simonson, J. M.; Mesmer, R. E. Solvation in High-Temperature Electrolyte Solutions. I. Hydration Shell Behavior from Molecular Simulation. *J. Chem. Phys.* **1999**, *110*, 1064–1074.

(49) Chialvo, A. A.; Chialvo, S.; Simonson, J. M.; Kalyuzhnyi, Y. V. Solvation phenomena in dilute multicomponent solutions I. Formal results and molecular outlook. *J. Chem. Phys.* **2008**, *128* (21), 214512.

(50) Chase, M. W., Jr.; Davies, C. A.; Downey, J. R., Jr.; Frurip, D. J.; McDonald, R. A.; Syverud, A. N. JANAF Thermochemical Tables. *J. Phys. Chem. Ref. Data* **1985**, *14*, 1 (supplement no. 1).

(51) The experimental setup has been built and tested, although the approach has not been fully implemented yet (for additional details see ref 3).

(52) Patra, M.; Karttunen, M. Systematic comparison of force fields for microscopic simulations of NaCl in aqueous solutions: Diffusion, free energy of hydration, and structural properties. *J. Comput. Chem.* **2004**, *25* (5), 678–689.

(53) Wang, J. M.; Cieplak, P.; Kollman, P. A. How well does a restrained electrostatic potential (RESP) model perform in calculating conformational energies of organic and biological molecules? *J. Comput. Chem.* **2000**, *21* (12), 1049–1074.

(54) Lindahl, E.; Hess, B.; van der Spoel, D. GROMACS 3.0: a package for molecular simulation and trajectory analysis. *J. Mol. Modell.* **2001**, *7* (8), 306–317.

(55) Aqvist, J. Ion-Water Interaction Potentials Derived from Free Energy Perturbation Simulations. *J. Phys. Chem.* **1990**, *94*, 8021–8024.

(56) Smith, D. E.; Dang, L. X. Computer Simulation of NaCl Association in Polarizable Water. *J. Chem. Phys.* **1994**, *100*, 3557–3566.

(57) Cole, D. R.; Chialvo, A. A.; Gruszkiewicz, M. S.; Palmer, D. A. *Thermophysical Properties Associated with Supercritical Coal-Fired Steam Generators*; ORNL: Oak Ridge, TN, 2007.

(58) Abascal, J. L. F.; Vega, C. A general purpose model for the condensed phases of water: TIP4P/2005. *J. Chem. Phys.* **2005**, *123* (23), 234505.

(59) Chialvo, A. A.; Cummings, P. T.; Simonson, J. M.; Mesmer, R. E. Temperature and Density Effects On The High Temperature Ionic Speciation in Dilute Na^+/Cl^- Aqueous Solutions. *J. Chem. Phys.* **1996**, *105*, 9248–9257.

(60) Guardia, E.; Marti, J.; Padro, J. Ion solvation in aqueous supercritical electrolyte solutions at finite concentrations: a computer simulation study. *Theor. Chem. Acc.* **2006**, *115* (2−3), 161–169.

(61) Sprik, M.; Ciccotti, G. Free Energy from Constrained Molecular Dynamics. *J. Chem. Phys.* **1998**, *109*, 7737–7744.

(62) Barthel, J. M. G.; Krienke, H.; Kunz, W. *Physical Chemistry of Electrolyte Solutions*; Springer: Darmstadt, 1998; Vol. 5.

(63) Wood, R. H.; Carter, R. W.; Quint, J. R.; Majer, V.; Thompson, P.; Boccio, J. R. Aqueous Electrolytes at High Temperatures: Comparison of Experiment with Simulation and Continuum Models. *J. Chem. Thermodyn.* **1994**, *26*, 225–249.

(64) Barthel, J.; Wachter, R.; Gores, H.-J. Temperature Dependence of Conductance of Electrolytes in Non-aqueous Solutions. In *Modern Aspects of Electrochemistry*; Conway, B. E., Bockris, J. O. M., Eds.; Plenum Press: New York, 1979; Vol. 13, pp 1−79.

(65) Barthel, J. Temperature Dependence of the Properties of Electrolyte Solutions. 1. Semi-Phenomenological Approach to an Electrolyte Theory Including Short-Range Forces. *Phys. Chem. Chem. Phys.* **1979**, *83*, 252–257.

(66) Fuoss, R. M. Paired ions: Dipolar Pairs as Subset of Diffusion Pairs. *Proc. Natl. Acad. Sci. U.S.A.* **1978**, *75*, 16–20.

(67) Bjerrum, N. Ionic Association. I. Influence of Ionic Association on the Activity of Ions at Moderate Degrees of Association. *K. Dan. Vidensk. Selsk., Mat. Fys. Medd.* **1926**, *7*, 1–48.

(68) Walther, J. V.; Schott, J. The Dielectric Constant Approach to Speciation and Ion Pairing at High Temperature and Pressure. *Nature* **1988**, *332*, 635–638.

(69) Conway, B. E. Factors Limiting Applications of the Historically Significant Born Equation. A Critical Review. In *Modern Aspects of Electrochemistry*; Conway, B. E.; White, R. E., Eds.; Kluwer Academic/Plenum Publishers: New York, 2002; Vol. 35, pp 295−323.

(70) Marshall, W. L. Solvent Structural Constant and Solvation Behavior Applied to the Description of Aqueous Electrolytes at 25−300 °C. *J. Chem. Soc., Faraday Trans. I* **1986**, *82*, 2283–2299.

(71) Ho, P. C.; Palmer, D. A.; Wood, R. H. Conductivity Measurements of Dilute Aqueous LiOH, NaOH, and KOH Solutions to High Temperatures and Pressures using a Flow-through Cell. *J. Phys. Chem. B* **2000**, *104*, 12084–12089.

(72) Bulemela, E.; Trevani, L.; Tremaine, P. R. Ionization constants of aqueous glycolic acid at temperatures up to 250 degrees C using hydrothermal pH indicators and UV-visible spectroscopy. *J. Solution Chem.* **2005**, *34* (7), 769–788.

(73) Takebayashi, Y.; Hotta, H.; Shono, A.; Otake, K.; Sue, K.; Yoda, S.; Furuya, T. Spectroscopic Study of Acid-base Equilibria and Ion Pairing in Supercritical Methanol. *J. Solution Chem.* **2009**, *38* (5), 545–555.

Received for review September 29, 2009. Accepted February 9, 2010. This research was sponsored by the Division of Chemical Sciences, Geosciences, and Biosciences, Office of Basic Energy Sciences under Contract No. DE-AC05-00OR22725 with Oak Ridge National Laboratory, managed and operated by UT-Battelle, LLC. Partial support from the Electric Power Research Institute (EPRI) is gratefully acknowledged.

JE900788R